Biocompatibility of Mussel-Inspired Water-Soluble Tissue Adhesives

Aishwarya V. Menon[1,2,†,*], Amelia A. Putnam-Neeb[2,†], Caitlin E. Brown[3,†], Christa J. Crain[4], Gert J. Breur[4,5], Sanjeev K. Narayanan[3,4], Jonathan J. Wilker[2,6,#,*], Julie C. Liu[1,7,#,*]

1. Davidson School of Chemical Engineering, Purdue University, West Lafayette, IN 47907, USA

2. Department of Chemistry, Purdue University, West Lafayette, IN 47907, USA

3. Department of Comparative Pathobiology, College of Veterinary Medicine, Purdue University, West Lafayette, IN 47907, USA

4. Center for Comparative Translational Research, Purdue University, West Lafayette, IN 47907, USA

5. Department of Veterinary Clinical Sciences, Purdue University, West Lafayette, IN 47907, USA

6. School of Materials Engineering, Purdue University, West Lafayette, IN 47907, USA

7. Weldon School of Biomedical Engineering, Purdue University, West Lafayette, IN 47907, USA

† Co-first author

 # Contributed equally as co-senior authors

** Corresponding author*

E-mail addresses: julieliu@purdue.edu (Julie C. Liu), wilker@purdue.edu (Jonathan J. Wilker), and menon54@purdue.edu (Aishwarya V. Menon)

Running Title: Biocompatibility of water-soluble glues

ABSTRACT

Wound closure in surgeries is traditionally achieved using invasive methods such as sutures and staples. Adhesion-based wound closure methods such as tissue adhesives, sealants, and hemostats are slowly replacing these methods due to their ease of application. Although several chemistries have been developed and used commercially for wound closure, there is still a need for better tissue adhesives from the point of view of toxicity, wet-adhesion strength, and long-term bonding. Catechol chemistry has shown great promise in developing wet-set adhesives that meet these criteria. Herein, we have studied the biocompatibility of a catechol-based copolymer adhesive, poly{[dopamine methacrylamide]-co-[methyl methacrylate]-co-[poly(ethylene glycol) methyl ether methacrylate]} or poly(catechol-MMA-OEG), which is soluble in water. The adhesive was injected subcutaneously in a mouse model on its own and in combination with a sodium periodate crosslinker. After 72 hours, 4 weeks, and 12 weeks, the mice were euthanized and subjected to histopathological analysis. Both adhesives were present and still palpable at the end of 12 weeks. The moderate inflammation observed for the poly(catechol-MMA-OEG) cohort at 72 h had reduced to mild inflammation at the end of 12 weeks. However, the moderate inflammatory response observed for poly(catechol-MMA-OEG) + crosslinker cohort at 72 h had not subsided at 12 weeks.

KEYWORDS

bioadhesives; biomimetic glues; histotoxicity; non-toxic glues; surgical glues

1. INTRODUCTION

Closure of both external and internal wounds in most surgeries around the world is traditionally achieved using sutures or staples. However, these wound closure methods cause damage to healthy tissue and can lead to discomfort, pain, itching, bacterial infections, and leakage of body fluids. Moreover, these techniques are often not applicable in modern minimally invasive and microsurgical procedures. In the past decade, alternative methods of wound closure such as hemostatic agents, sealants, and adhesives have been developed to replace traditional wound closure methods.[1–4] The key requirements for such adhesion-based wound closure methods include an ability to adhere to tissues in wet environments, biocompatibility, and degradability into non-cytotoxic by-products.

Various chemistries have proven to be useful in wound closure, including fibrin protein, cyanoacrylates (e.g., Dermabond), aldehyde crosslinking chemistry, *N*-hydroxysuccinimide (NHS) reactive esters, and polyurethanes.[2,5] However, each category has some drawbacks such as weak adhesion in wet environments or toxicity. Biomimetic catechol- and gallol-based chemistries have been explored for wet-tissue adhesion. The inspiration for these adhesives comes from sea animals such as mussels and barnacles that produce adhesive proteins for attachment onto surfaces in wet and dynamic sea environments.[6–9] The key component of these adhesive proteins is the amino acid 3,4-dihydroxyphenylalanine (DOPA), which has a pendant catechol functional group that is responsible for crosslinking and adhesion chemistry. Biomimetic wet tissue adhesives can be synthesized by tethering this catechol functional group onto several different polymeric host systems.[10–13]

Our research groups have previously made such mussel-mimetic adhesives by incorporating catechol groups in synthetic polymer systems such as polystyrene[14–16] and polylactic acid,[17–19] as well as in bioinspired proteins such as elastin-like polypeptides (ELP).[20–22] One such biomimetic wet adhesive was synthesized by copolymerizing methyl methacrylate (MMA), poly(ethylene glycol) methyl ether methacrylate monomers, and dopamine methacrylamide (DMA) to provide a catechol group for adhesion (Figure 1a).[23,24] The resulting polymer, poly{[dopamine methacrylamide]-co-[methyl methacrylate]-co-[poly(ethylene glycol) methyl ether methacrylate]}, was named poly(catechol-MMA-OEG). The design intent was to create a biomimetic adhesive with high strength and tunable ductility due to the incorporation of both stiff MMA groups and lower modulus, flexible oligoethylene glycol (OEG) groups. Thus, poly(catechol-MMA-OEG) was designed as a biomimetic adhesive with improved mechanical properties compared to catechol with either only OEG or only poly(methyl methacrylate) (PMMA). Previously, we studied the adhesion strength of this biomimetic polymer on metal and plastic substrates by varying the ratio of incorporation of the monomers. The highest adhesion strength was obtained on aluminum substrates when ~45 mol% OEG was incorporated. The adhesion strength was slightly lower than most commercial glues (i.e., cyanoacrylate, epoxy, and poly(vinyl acetate)).[23] In another study where the mole percentage of catechol incorporation was varied, ~10 mol% catechol yielded the highest strengths when using aluminum substrates.[24] Although this ideal composition of poly(catechol-MMA-OEG) is still not as strong as common structural adhesives, other applications such as biomedical adhesives may look more promising given the desirable mechanical properties and the relatively low toxicity of the polymer backbone.

Poly(methyl methacrylate) is commonly used in intraocular lenses, bone cement, and dentistry due to its mechanical strength and low toxicity.[25–27] Poly(ethylene glycol) (PEG) (as well as OEG) is non-toxic, nonimmunogenic, biocompatible, and has been approved by the United States Food and Drug Administration (FDA) for use in the biomedical industry.[28–30] The added ductility from OEG is beneficial because tissue adhesives and sealants will ideally have similar moduli to the surrounding soft tissues in the body. Additionally, the optimal ratio of monomers in this system allows for solubility in water without the need for potentially toxic organic solvents. Crosslinkers with an oxidizing nature such as iron salts and periodate are added to catechol-containing polymers to enhance their adhesion strengths.[31] Therefore, sodium periodate was chosen as a crosslinker for the poly(catechol-MMA-OEG) system studied here.

Wanting to investigate clinical suitability, we studied the biocompatibility of poly(catechol-MMA-OEG) adhesive and adhesive + crosslinker system via subcutaneous injection in mice after 72 h, 4 weeks, and 12 weeks. Five mice were studied in each experimental group. We found no evidence of *in vivo* systemic toxicity in any of the mice during the entire duration of the study. All the animals injected with poly(catechol-MMA-OEG) alone showed a mild inflammatory response at all the studied time points. The mice injected with poly(catechol-MMA-OEG) + crosslinker showed slightly more inflammation.

2. MATERIALS AND METHODS

2.1 Overall study design

The protocol for the animal study was reviewed and approved by the Purdue Animal Care and Use Committee (protocol no: 1701001532A001). For the studies, test articles were injected subcutaneously into healthy female CD-1 mice (weighing 18-20 g) for clinical and histological evaluation based on standards for biological evaluation of medical devices (ISO 10993, Part 1, 2, 6, 10, and 11).[32–36] Two test articles were evaluated: poly(catechol-MMA-OEG) and poly(catechol-MMA-OEG) + crosslinker. For each experimental group, mice (n=5) were injected with one of the test articles in a dorsolateral location (left or right side randomly chosen) and with an equal volume of saline control contralaterally. Each test article was examined at the three different time points of 72 h, 4 weeks, and 12 weeks (Figure 1b). The number of mice to be studied per experimental group was chosen based on the recommended minimum group sizes to obtain meaningful results (ISO 10993, Part 2 and 11).[32,36] After injection, the mice were observed for systemic and local adverse reactions. The mice were euthanized through inhalation of carbon dioxide mixed with isoflurane followed by creation of pneumothorax. After euthanasia, the tissue around the injection site and all major organs were examined via histology.

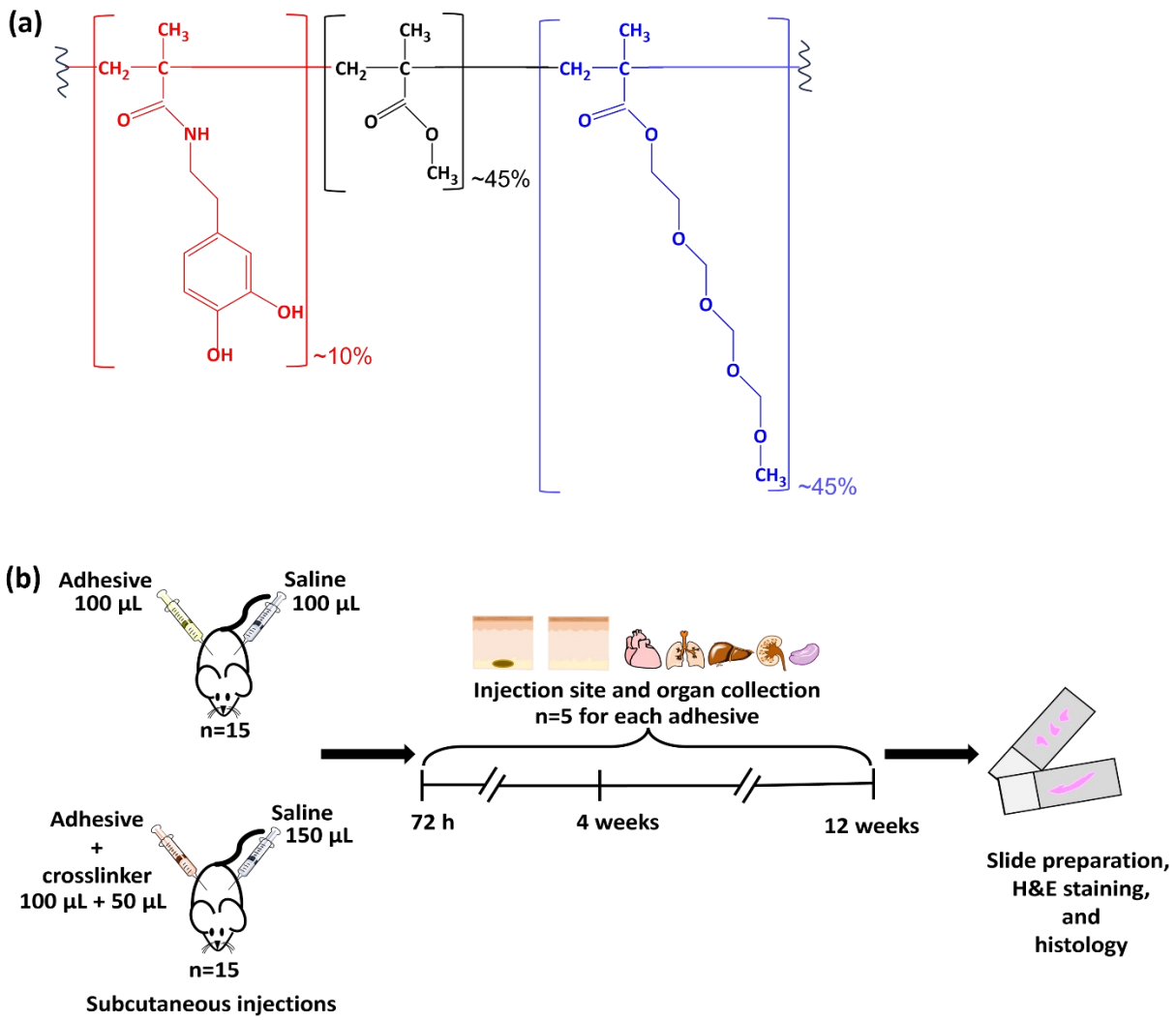

Figure 1: (a) Structure of poly(catechol-MMA-OEG) adhesive used in this study. (b) Overview of experimental design involving subcutaneous injection of poly(catechol-MMA-OEG) and poly(catechol-MMA-OEG) + crosslinker in mice.

2.2 Materials

All of the reagents used in this study were obtained from Sigma-Aldrich unless stated otherwise.

2.3 Adhesive and crosslinker preparation

Poly{[dopamine methacrylamide]-co-[methyl methacrylate]-co-[poly(ethylene glycol) methyl ether methacrylate]}, or poly(catechol-MMA-OEG), was synthesized via polymerization of dopamine methacrylamide, methyl methacrylate, poly(ethylene glycol) methyl ether methacrylate monomers with 2,2-azobis(2-methyl propionitrile) (AIBN) in *N, N*-dimethylformamide (DMF).[23,24] DMA was synthesized and characterized as per literature methods.[23,24,37] The catechol content for optimum adhesion strength was found to be ~10 mol% and therefore was chosen for this study.[24] The percent incorporation of OEG and MMA was ~45 mol% each. Sodium periodate was used as a crosslinker for the poly(catechol-MMA-OEG) system.

Poly(catechol-MMA-OEG) was dissolved at a concentration of 10% (w/v) in water. Sodium periodate ($NaIO_4$) was dissolved in water at a crosslinker (IO_4^-) to catechol ratio of 1:3. Crosslinker concentration was calculated prior to preparation to deliver 50 µL of crosslinker solution with 100 µL of adhesive solution. For sterilization, the poly(catechol-MMA-OEG) adhesive system was dissolved in water at 10% (w/v) and autoclaved for 30 min with a fluid cycle, and the adhesive was allowed to redissolve overnight under nitrogen prior to injection. The crosslinker solution was sterilized by passing through a 0.22 µm sterile polytetrafluoroethylene (PTFE) filter into a sterile injection vial.

2.3 Injection of test articles

The mice were kept under general anesthesia (isoflurane) and were injected with the sterilized adhesive solutions subcutaneously. For adhesive alone, 100 µL of the adhesive was injected subcutaneously in a dorsolateral location, and 100 µL of a saline control was injected contralaterally. For adhesives with crosslinker, an 18-gauge needle was inserted subcutaneously

and held in place while inserting a 22-gauge needle through the lumen of the 18-gauge needle. First, 100 µL of the adhesive was injected through the 22-gauge needle, after which the 22-gauge needle was removed. Next, 50 µL of the crosslinker solution was injected through the remaining 18-gauge needle into the same location. This method allowed the adhesive and crosslinker to mix *in vivo* since it crosslinked almost instantly. When the adhesive + crosslinker combination was injected, the amount of saline injected contralaterally was 150 µL.

2.4 Observation of systemic effects

The mice were observed for any signs of anaphylactic shock immediately after injection. Further, they were kept under observation for 24, 48, and 72 h after injection. The activity level and body weight of the mice were also recorded as per ISO 10993 Part 11 to test for systemic toxicity.[32] The body weights were recorded prior to injection and once per week post-injection. The organs (i.e., liver, kidneys, spleen, heart, and lungs) were histopathologically evaluated for toxicity, but no specific grading scheme was employed. Organs were preserved in 10% neutral buffered formalin at necropsy. The tissues were further processed and embedded in paraffin for sectioning and stained with hematoxylin and eosin (H&E) or Masson's Trichrome (MTC). The representative microscopic images were captured using an Olympus DP25 digital camera mounted on an Olympus BX41 microscope. All histological analyses were performed by two blinded board-certified veterinary pathologists.

2.5 Observation of local effects

A scoring system based on ISO 10993 Part 10 was used to test for signs of irritation and skin sensitization around the injection site.[33] Mice were inspected for signs of erythema after 2, 4, and 6 h post-injection, every 24 h for 7 days, and then once a week for the remainder of the

animal study. The palpability of the injected adhesives was noted weekly and at the time of necropsy to check for any adhesive resorption. Postmortem, the injection site was processed as described in the previous section and histopathologically evaluated based on a semi-quantitative scoring system (ISO 10993 Part 6).[34] A scale of 0 to 4 (0 indicated no reaction, 1 indicated minimal reaction, 2 indicated mild reaction, 3 indicated moderate reaction, and 4 indicated severe reaction) was used to evaluate H&E and MTC stained slides.

2.6 Statistics

Statistical analysis was performed using non-parametric tests in JMP software. When comparing only two groups (adhesive and adhesive + crosslinker), the Wilcoxon test was used with $\alpha = 0.05$. When comparing more than two groups (72 h, 4 weeks, and 12 weeks), the Steel-Dwass test was used with $\alpha = 0.05$. Statistical significance is indicated by a * symbol such that groups that are marked with * are statistically different ($p < 0.05$).

3. RESULTS

3.1 *In vivo* effects

No adverse systemic reactions were seen. None of the mice showed an adverse reaction immediately following injection. All mice maintained their body weight during the study period, and no abnormal behavior or lethargy was observed.

None of the mice injected with either of the adhesives showed any signs of erythema at the injection sites and had minimal irritation. Both poly(catechol-MMA-OEG) and poly(catechol-MMA-OEG) + crosslinker were still palpable in all mice and could be harvested at necropsy even after 4 and 12 weeks.

3.2 Histology of mice injected with poly(catechol-MMA-OEG)

3.2.1 Histology of injection site

Figure S1a shows the comparison of a typical injection site injected with only saline (Figure S1a) versus adhesives (Figure S1b and Figure S1c) at 12 weeks. The sites injected with saline showed clearly visible skin layers (e.g., epidermis, dermis, and hypodermis) with no inflammation whereas the sites injected with adhesives showed ensuing inflammation surrounding the adhesives. Tables S1-S3 show the scores for various types of inflammatory cells and inflammatory responses observed in individual mice injected with poly(catechol-MMA-OEG) at various time points.

A more detailed histological examination showed that the injection site for poly(catechol-MMA-OEG) after 72 h was characterized by the presence of heavy macrophagic infiltration, moderate granulation tissue, and mild to moderate fibrosis (Figures 2a-c). Severe macrophage infiltration, which appeared as a high density of blue-colored round/oval basophilic cells surrounding the adhesive, was observed at 72 h (Figure. 2a) but was reduced substantially in the 4 (Figure 2b) and 12 week (Figure 2c) cohorts. No significant changes in granulation tissue and fibrosis scores were observed at 4 and 12 weeks (Figure 2d). The adhesive present at 12 weeks was also occasionally lightly basophilic, which suggested mild mineralization. The transition of granulation tissue to fibrosis and reduced macrophages suggest a resolution of the inflammatory process. Additionally, multinucleated cells were found at all three time points, and neutrophils reduced significantly at 4 weeks and were nonexistent at 12 weeks. Plasma cells and lymphocytes were present at all time points. Eosinophils were found in all mice at all time points. No signs of necrosis were observed at any of the studied time points. A translucent material, consistent with

the colorless and transparent poly(catechol-MMA-OEG), was present at the center of fibrosis and inflammation at all three time points. The surface of the adhesive appeared rougher and there was an increase in inflammatory cell infiltration with each studied time point (Figure S2). These observations could suggest possible mild degradation of the adhesive with the passage of time.

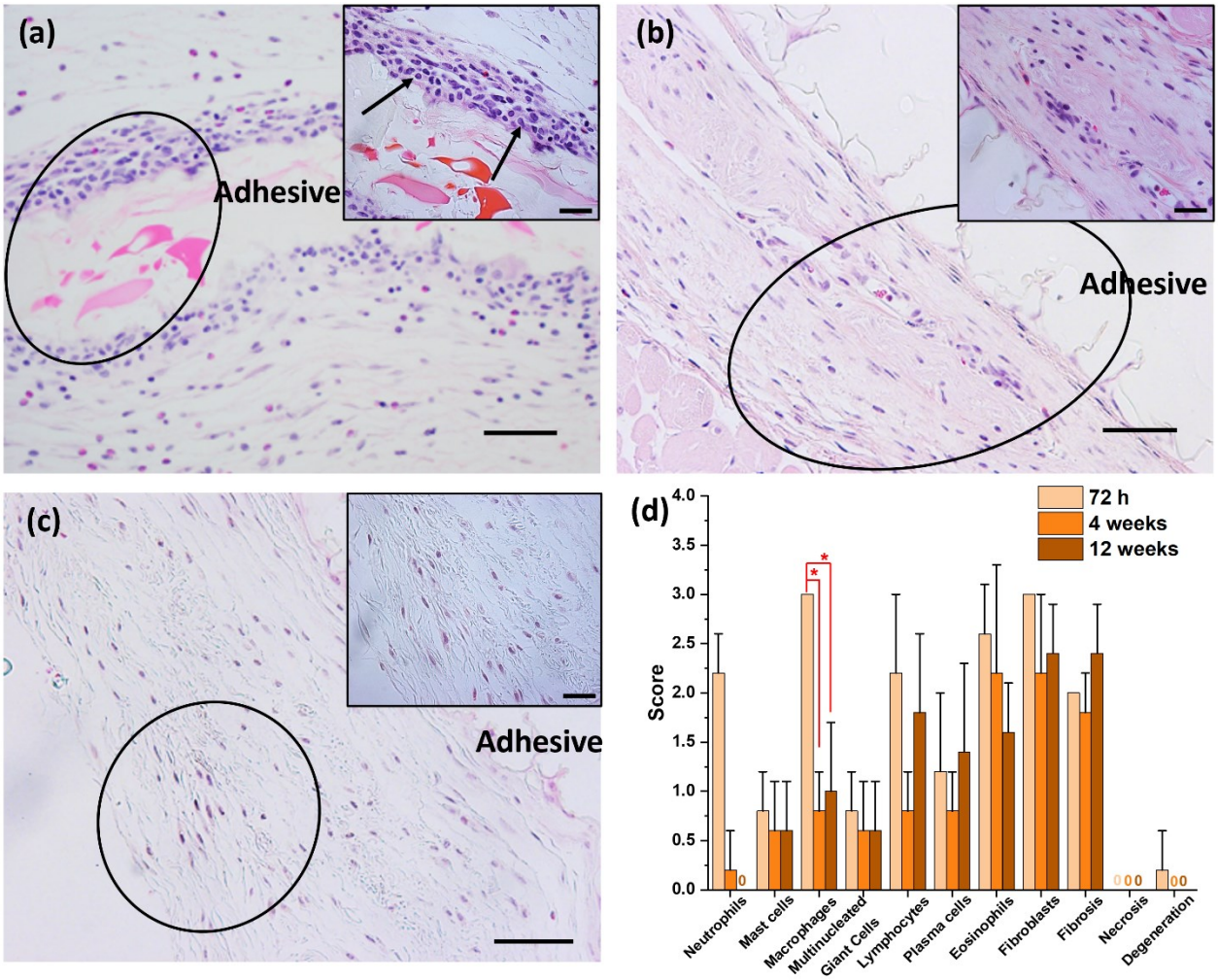

Figure 2: The histology of the injection site for poly(catechol-MMA-OEG) was characterized by the presence of eosinophils, neutrophils, lymphocytes, and macrophages around the transparent adhesive material. **(a)** Heavy macrophage infiltration around the adhesive (indicated by black arrows) was observed at 72 h but was reduced substantially at **(b)** 4 weeks and **(c)** 12 weeks. The inset shows higher magnification images of the corresponding low-magnification areas indicated by the black circle. Scale bars represent 50 µm and 25 µm for low and high (figures in inset) magnification images, respectively. **(d)** Graph showing average scores of all histological findings. * represents statistical significance with $p < 0.05$.

To further evaluate the presence of fibroplasia/fibrosis around the adhesive materials, MTC staining was pursued. Table S4 shows the individual MTC scores for all mice injected with adhesive alone. Low-magnification images show the presence of a dense band of fibroblasts and mature collagen at all time points (Figures 3a-c). The amount of collagen surrounding the adhesive at 72 h increased at 4 weeks (Figure 3d). There was no significant increase in the amount of collagen at 12 weeks. These findings signified that the adhesive material was completely walled off by fibrosis (mature fibroblasts and collagen) within 4 weeks.

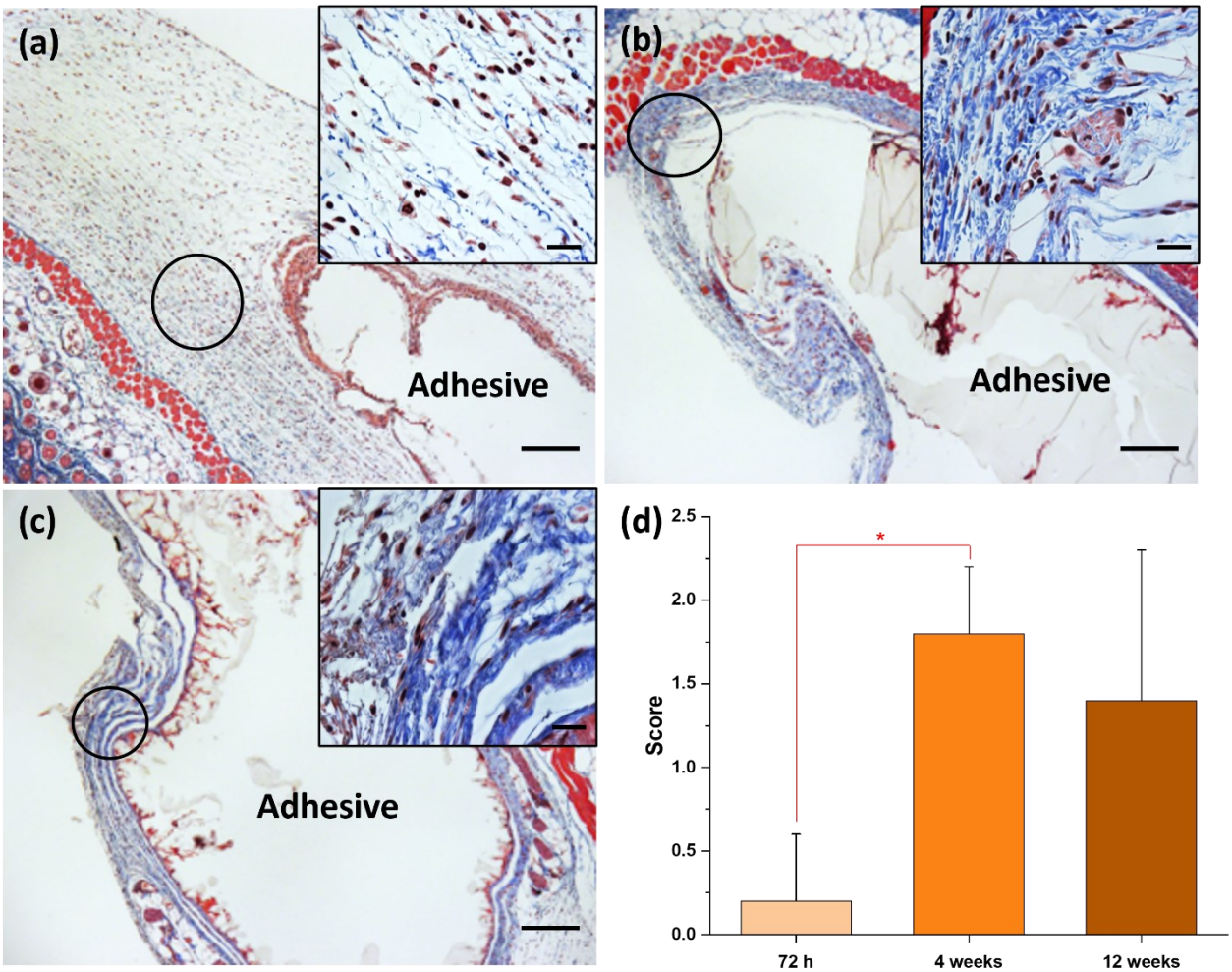

Figure 3: A dense collagenous band, composed of fibroblasts (nuclei, brown) and collagen (blue), formed around poly(catechol-MMA-OEG), and the adhesive material was completely walled off within 4 weeks. Low magnification images showing fibroblasts (nuclei, brown) and collagen (blue-colored fibrils) surrounding the adhesive at **(a)** 72 h increased substantially at **(b)** 4 weeks and **(c)** 12 weeks. The inset shows higher magnification images of the corresponding low-magnification areas indicated by the black circle. Scale bars represent 200 µm and 25 µm for low and high (figures in inset) magnification images, respectively. **(d)** Graph showing average MTC stain scores for mice at all time points. * represents statistical significance with $p < 0.05$.

3.2.2 Histology of organs

In the 72 h cohort, small multifocal areas of corticomedullary congestion and hemorrhage (represented by dark pink to red staining within the black ovals) were observed in the kidneys for 2 out of 5 mice (Figure 4a). The renal congestion and hemorrhage were present in 2 out of 5 mice at 4 weeks (Figure 4b) and 4 out of 5 mice at 12 weeks (Figure 4c). The liver of one of the mice in the 4 week cohort contained a focal area of necrosis (represented by dark pink staining in the yellow marked region) accompanied by infiltration of neutrophils, macrophages, and a few eosinophils (Figure 4d). All other organs including the heart, lungs, and spleen were histologically normal in all mice, at all of the studied time points.

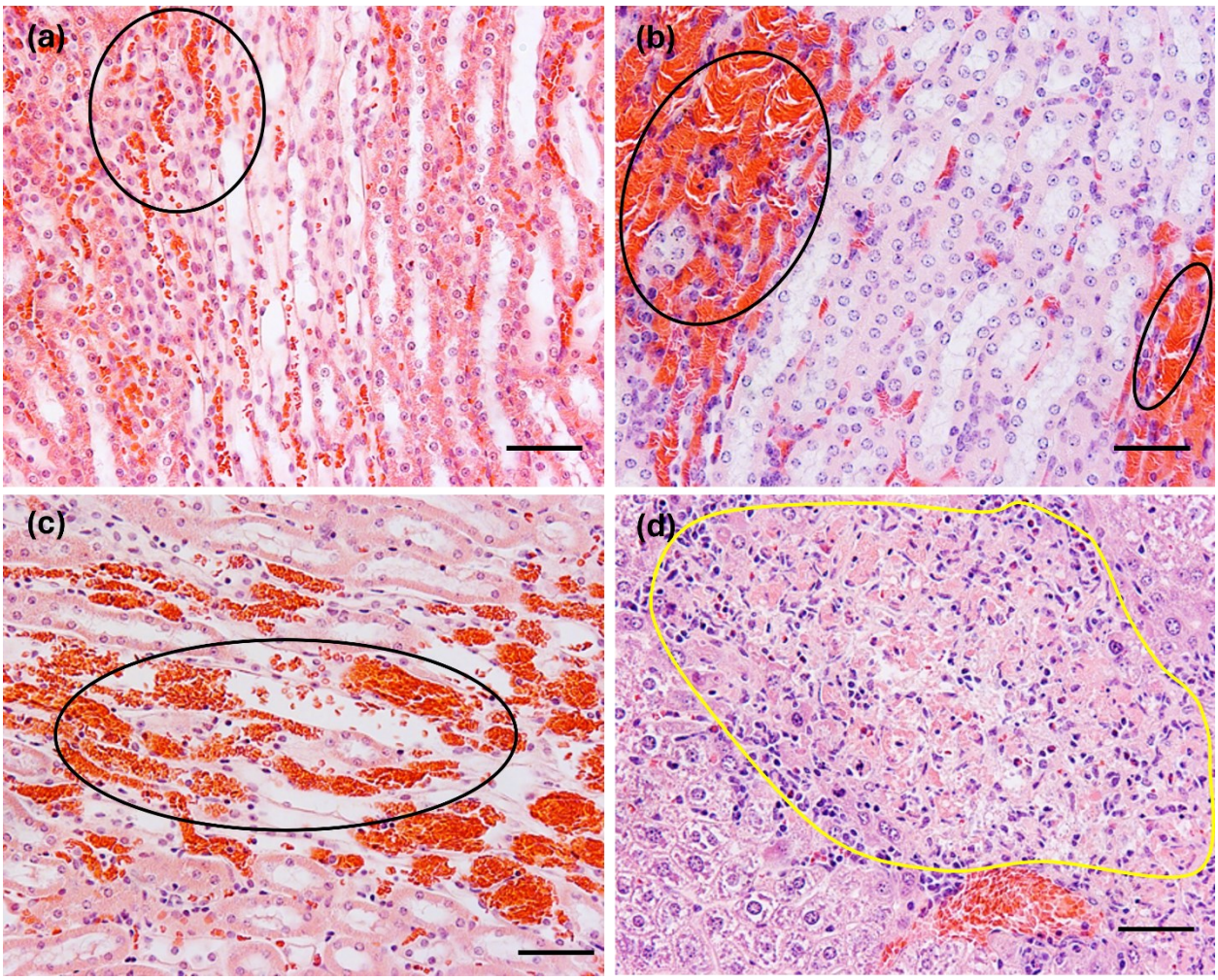

Figure 4: Small multifocal areas of hemorrhage and congestion (indicated by black ovals) were observed in the corticomedullary junctions of the kidneys of a subset of the poly(catechol-MMA-OEG) cohort at **(a)** 72 h, **(b)** 4 weeks, and **(c)** 12 weeks. **(d)** The liver in one mouse of the 4 week cohort was characterized by small focal areas of necrosis and infiltration of inflammatory cells (within the yellow marked area). Scale bars represent 50 µm.

3.3 Histology of mice injected with poly(catechol-MMA-OEG) + crosslinker

3.3.1 Histology of injection site

Tables S5-S7 show the scores for different inflammatory cells and inflammatory responses observed in mice injected with poly(catechol-MMA-OEG) + crosslinker at various time points. For the poly(catechol-MMA-OEG) + crosslinker group, heavy macrophage infiltration, moderate granulation tissue, and mild to moderate fibrosis were consistently observed at all time points (Figures 5a-c). Neutrophils and plasma cells were present at 72 h and did not decrease at 4 and 12 weeks (Figure 5d). This observation may suggest a chronic inflammatory response. Eosinophils were also present at all time points and indicated a prolonged hypersensitivity reaction. Lymphocytes present at 72 h decreased slightly at 4 weeks. Multinucleated giant cells were not present at 72 h but were found at 4 and 12 weeks. No signs of necrosis were observed at any of the studied time points. The poly(catechol-MMA-OEG) + crosslinker system was still present in the dermis at 12 weeks. The colorless material in the center of inflammation at 72 h had areas of slightly pink mineralized material at 4 weeks and areas with complete mineralization (indicated by the dark pink to purple coloration of the adhesive) at 12 weeks (Figure 5c). Similar to mice injected with adhesive alone, an increase in the surface roughness of the adhesive + crosslinker accompanied by increased infiltration of inflammatory cell was observed with the passage of time (Figure S3).

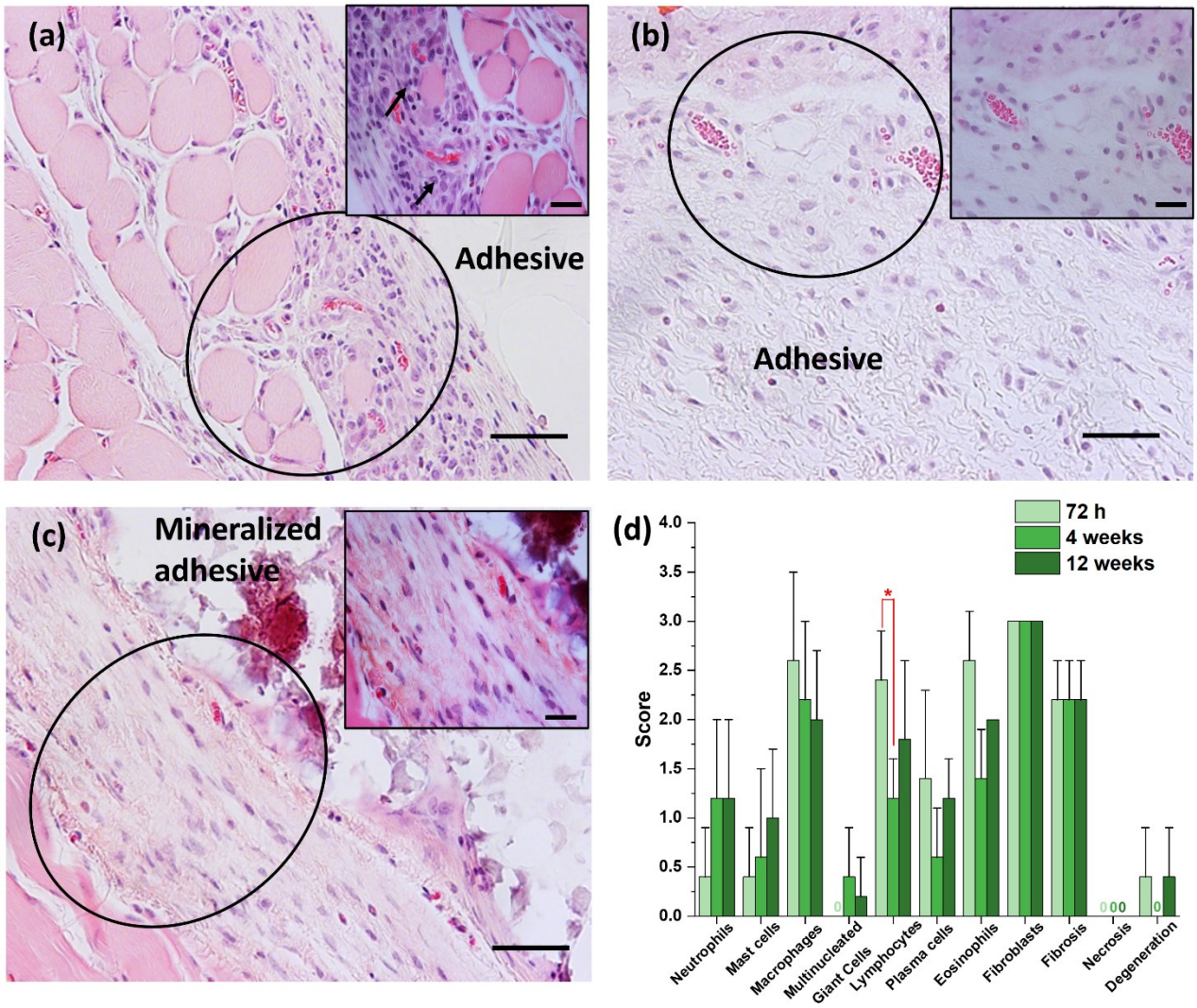

Figure 5: Histology of the poly(catechol-MMA-OEG) + crosslinker cohort was characterized by the presence of eosinophils, neutrophils, lymphocytes, and macrophages. Figure shows the presence of inflammatory cells around the transparent adhesive material at **(a)** 72 h (macrophages indicated by black arrows), **(b)** 4 weeks, and **(c)** 12 weeks. The adhesive appeared mineralized at 12 weeks (indicated by dark pink to purple coloration of the adhesive). The inset shows higher magnification images of the corresponding low-magnification areas indicated by the black circle. Scale bars represent 50 µm and 25 µm for low and high (figures in inset) magnification images,

respectively. **(d)** Graph showing average scores of all histological findings. * represents statistical significance with $p < 0.05$.

Table S8 shows the individual MTC scores for all mice injected with adhesive + crosslinker. Low-magnification images of MTC-stained tissue sections showed the presence of a collagenous network at all time points (Figures 6a-c). The amount of collagen formed around the adhesive increased at 4 weeks with no significant increase at 12 weeks (Figure 6d). This trend was similar to that observed for the adhesive-only system. Here, too, the adhesive material was completely walled off within 4 weeks.

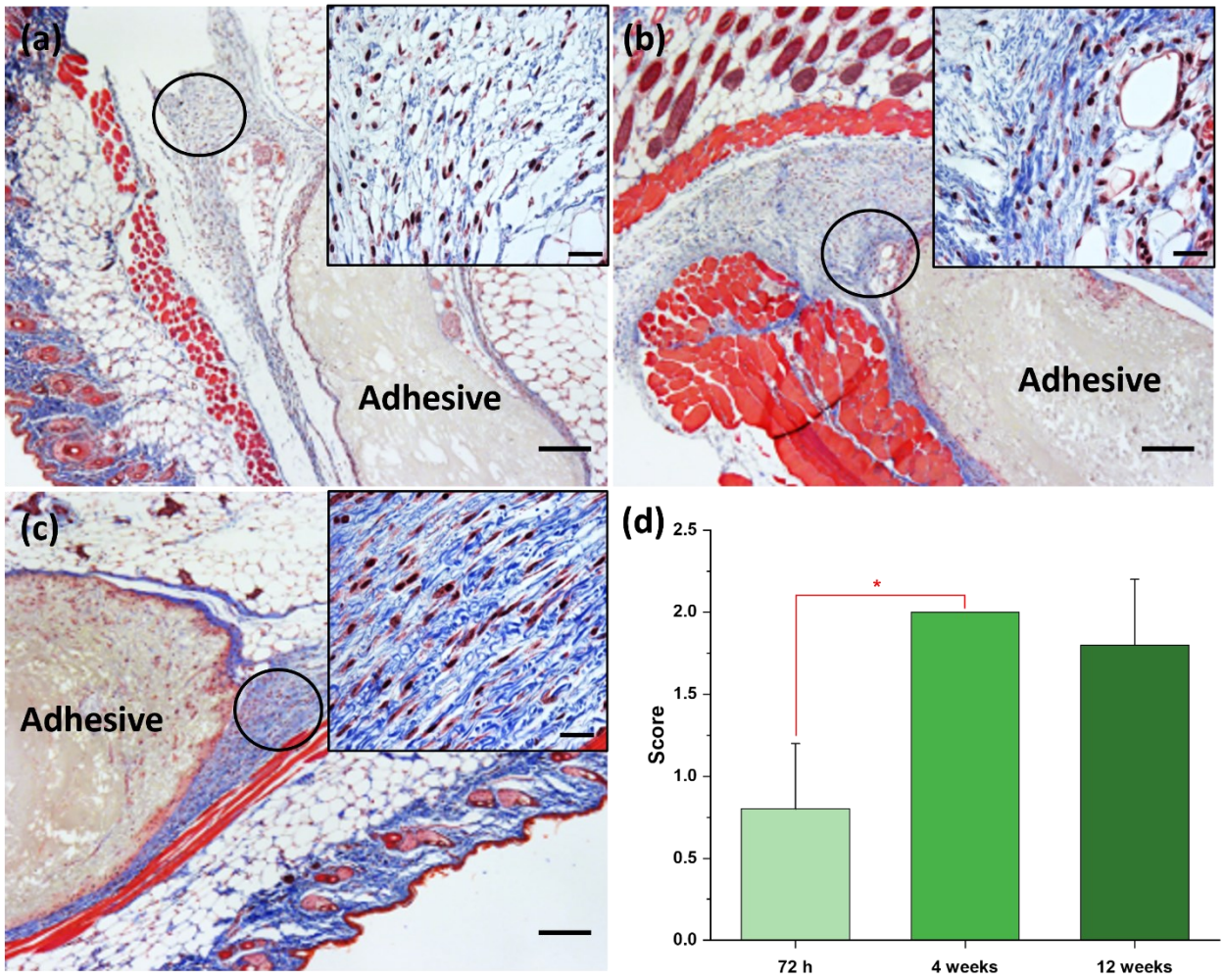

Figure 6: Similar to the adhesive only, a collagenous network formed around the poly(catechol-MMA-OEG) + crosslinker adhesive and completely walled it off within 4 weeks. Low magnification images showing a fibrous network (blue-colored fibrils) that had formed around the adhesive at **(a)** 72 h and increased substantially at **(b)** 4 weeks and **(c)** 12 weeks. The inset shows higher magnification images of the corresponding low-magnification areas indicated by the black circle. Scale bars represent 200 µm and 25 µm for low and high (figures in inset) magnification images, respectively. **(d)** Graph showing average MTC stain scores for mice at all time points. * represents statistical significance with $p < 0.05$.

3.3.2 Histology of organs

Multifocal corticomedullary congestion in the kidneys was observed in one of the mice in the 72 h cohort (highlighted by the black oval in Figure 7a), two of the mice in the 4-week cohort, and 4 out of 5 mice in the 12-week cohort. Similar congestion was also observed in some mice injected with adhesive alone. Further, at 12 weeks, the kidney of one of the mice was characterized by multifocal interstitial lymphoplasmacytic nephritis (highlighted by the black oval in Figure 7b) in addition to the observed corticomedullary congestion. The livers in all of the mice were histopathologically normal with mild vacuolar hepatopathy observed in all mice. However, at 12 weeks, multifocal regions of lymphoplasmacytic hepatitis were observed in the liver of one of the mice as seen in the black oval in Figure 7c. All other organs including the heart, lungs, and spleen were histologically normal.

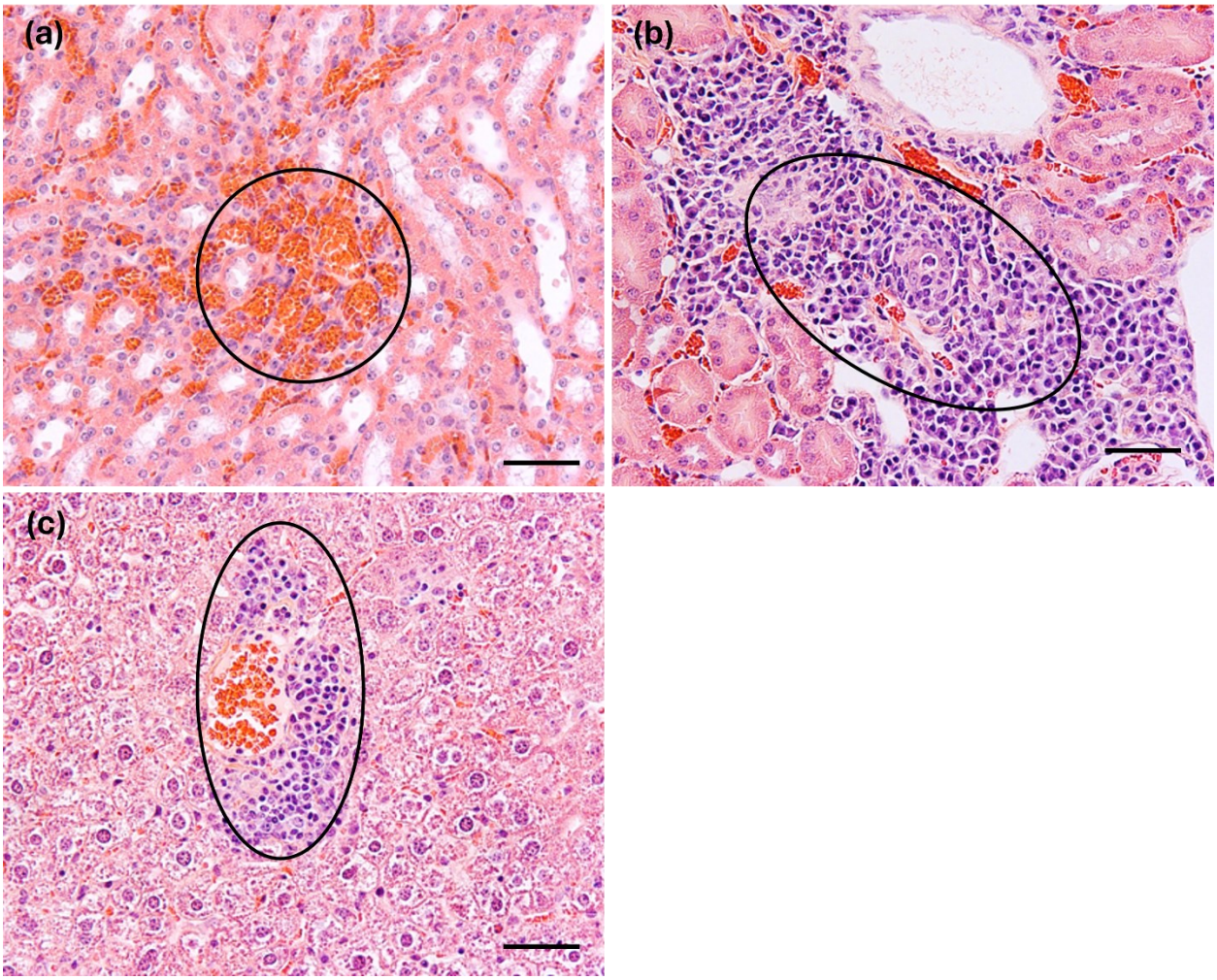

Figure 7: Similar to the mice injected with poly(catechol-MMA-OEG) alone, the mice injected with poly(catechol-MMA-OEG) + crosslinker indicated renal congestion. **(a)** The kidneys of the 72 h cohort were characterized by multifocal corticomedullary congestion as indicated by the circled area. **(b)** Multifocal interstitial lymphoplasmacytic nephritis of the kidney was observed in one mouse at 12 weeks. **(c)** Lymphoplasmacytic hepatitis in the liver of one mouse from the 12-week cohort is indicated by the marked area. Scale bars represent 50 µm.

4. DISCUSSION

The purpose of this study was to determine inflammatory response and subsequent biocompatibility when a foreign substance, such as our synthetic tissue adhesive, was injected, and therefore the biocompatibility of our adhesive systems was compared against a negative control (saline). Saline[38,39] or phosphate-buffered saline[40–43] has extensively been used as a negative control to compare and determine the biocompatibility of biomaterials due to their negligible tissue response upon injection.

Mussel-inspired water-soluble adhesives were synthesized and subcutaneously injected in healthy mice to study their suitability for biomedical applications. None of the mice had systemic or adverse *in viv*o reactions. All mice injected with the adhesive showed a severe macrophage infiltration around the injectate at all time points. However, for mice injected with adhesive alone, moderate macrophage infiltration at 72 h reduced significantly by 4 and 12 weeks. Mice injected with adhesive + crosslinker did not show significant reduction in macrophages at 12 weeks. However, no necrosis of the injected sites were observed for either of the adhesive systems at any of the studied time points. Both the adhesives were successfully walled off within 4 weeks, and the fibrosis (fibroblasts and mature collagen) present around both adhesive systems proceeded similarly at all the studied time points. At all time points, some mice from both groups had congestion and local hemorrhage of the kidney. The total number of mice exhibiting renal congestion per time point increased in the case of both adhesives (4 out of 5 for both adhesives by 12 weeks). The clinical significance of this finding is unknown; however, there was no apparent histologic effect on the surrounding renal parenchyma, and all animals survived their scheduled necropsy.

Developing adhesives for biomedical applications is challenging since it involves balancing biocompatibility, adhesive performance, and adhesive stiffness. Poly(catechol-MMA-OEG) was specifically designed to tune the polymer mechanical properties by altering the ratio of stiff methyl methacrylate (MMA) groups and soft oligo(ethylene glycol) (OEG) groups to achieve a material with high strength and ductility.[23,24] Although the highest adhesion strength with aluminum substrates was obtained when dichloromethane (DCM) was used to dissolve poly(catechol-MMA-OEG), there was concern about the toxicity of DCM *in vivo*. Thus, we focused on formulations using water as the solvent. However, the lowest adhesion strength was obtained when water was the solvent,[24] and poly(catechol-MMA-OEG) with 10 mol% catechol and 45 mol% OEG was soluble in water only at a low concentration of 10% (w/v). Thus, for biomedical applications, where biocompatibility is a concern, there is an inherent tradeoff with this system between higher bonding strengths and lower toxicity.

To place our study in context, we compared our results to studies that examined various components of our copolymer systems as part of their adhesive formulation. First, PEG has been used in many biomedical materials and was not expected to contribute to the inflammatory response seen in our study. Polyethylene glycol-based tissue adhesives are currently used in commercial products such as FocalSeal, DuraSeal, CoSeal, Resure, and Adherus for dural, pleural, vascular, and ocular repair surgeries.[2,44] Although these adhesives are used within the body without adverse side effects, they suffer from other drawbacks such as poor mechanical properties and swelling, which can lead to post-surgical complications including nerve compression.[45,46] Brubaker et al. developed mussel-inspired PEG-based hydrogels by functionalizing branched PEG with catechol.[47] The hydrogel was subcutaneously placed in mice

and observed for up to 1 year.[47] Minimal inflammatory cell infiltration was seen at short implantation times of 1 and 6 weeks. Moreover, the hydrogel was still present at the implantation site one year post-implantation. Even when the hydrogel was modified with protease sites to facilitate degradation, the material only had mild bulk degradation after 16 weeks as denoted by increased surface roughness and changes in the original geometry of the material.[48] Our findings are consistent with these prior results in that poly(catechol-MMA-OEG) was still palpable and an increase in the surface roughness of the injected adhesives was observed at 12 weeks (Figure S2 and S3). Additionally, these prior results suggest it is unlikely that the PEG component of the copolymer adhesive contributed to the observed foreign body response.

Poly(methyl methacrylate) is often used in bone cement and its polymerized form is not cytotoxic; however, the unpolymerized monomeric form (MMA) has proven local and systemic effects including cell and tissue toxicity. Furthermore, the exothermic polymerization reaction leads to thermal necrosis.[49] Poly(methyl methacrylate)-based bone cement has also been reported to cause a foreign body response that manifests as a giant cell foreign body granulomatous reaction.[50] Suzuki et al. studied the biocompatibility of a PMMA-based tissue adhesive composed of 4-methacryloyloxyethyl trimellitate anhydride and MMA monomers, tri-*n*-butylborane for an initiator, and PMMA powder for a filler.[51] When applied to full-thickness abdominal incision wounds in rats, the wounds healed with mild granulation tissue at deeper layers of skin after three months. Clinical studies have also shown that unreacted MMA can cause adverse effects such as liver toxicity and irritation to skin, eyes, and mucous membranes.[52] Therefore, the FDA has mandated that the monomer levels in medical grade PMMA should be less than 1% in intraocular lenses.[53] In our case, it is unlikely that any significant amounts of

unreacted MMA monomer would be present in the adhesive at the time of injection since sterilization of poly(catechol-MMA-OEG) via autoclaving should polymerize any unreacted monomer.

However, degradation of the adhesive into smaller molecules either by hydrolysis or enzymatically over 12 weeks or during autoclaving cannot be ruled out. Low-magnification images of the injection sites (Figures S2 and S4) showed signs of foreign body reaction around the adhesive. Inflammatory cell enzymes released due to foreign body reactions could lead to potential bulk degradation of the adhesive over time. Therefore, it is possible that the renal congestion and mild liver necrosis observed in mice in this study may have been caused by adhesive degradation products. The total number of mice exhibiting renal congestion increased over the course of time and may support our hypothesis that leaching of adhesive degradation products over time could be the reason for these observed kidney and liver pathologies.

Incorporating catechol within polymers has been found to result in a stronger foreign body reaction and an increased macrophage infiltration compared to the base polymer alone.[54] One limitation of this work is that macrophage phenotypes (M1 or M2) were not identified through immunohistochemical staining, so the specific stage of inflammation was not elucidated. The inflammatory response observed here was attributed to catechol autoxidation into the quinone form and subsequent generation of reactive oxygen species such as H_2O_2 and superoxide anion ($O_2^{\cdot -}$).[55,56] In our study, the inflammatory reaction observed at the injection site in the first couple of weeks could be a result of catechol oxidation in the adhesive.

Histological evaluation showed that the adhesive + crosslinker system generally exhibited higher numbers of infiltrated macrophages or neutrophils at later time points (4 and 12 weeks)

compared to the adhesive alone system (Figure 8). The adhesive + crosslinker system could therefore be considered more immune stimulatory than the adhesive alone. Moreover, mineralization of the adhesive at the injection site was only observed when the adhesive + crosslinker system was injected. Sodium periodate is known to induce toxicity within the gastrointestinal tract and kidneys in rats when administered orally.[57] Periodate can oxidize catechol to promote adhesive crosslinking but can also oxidize RNA, glycoproteins (e.g., fibronectin), and glycosaminoglycans (e.g., hyaluronic acid). Upon application, strong oxidants, such as periodate ions (IO_4^-), are reduced to produce more stable and less reactive oxygen species (ROS), such as H_2O_2, which promotes a foreign body response and can continue to cause oxidative tissue damage that results in chronic wounds and complication in tissue repair.[58] Since the adhesive alone showed some resolution to the inflammatory response, continued oxidative damage could explain the chronic inflammatory response when the periodate crosslinker was added to the adhesive.

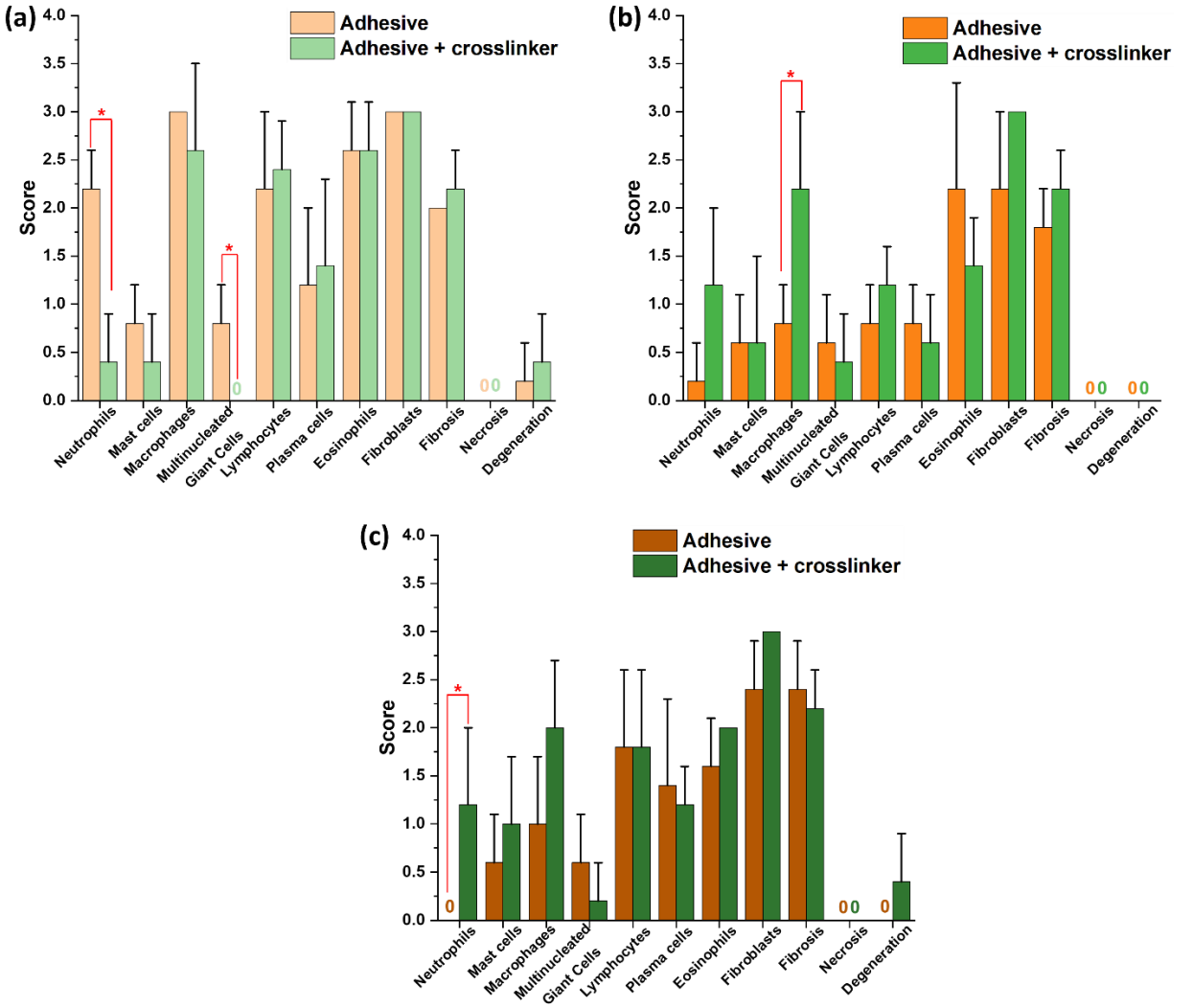

Figure 8: Histological evaluation showed that the adhesive + crosslinker system was more immune stimulatory than the adhesive alone. Figure showing differences in inflammatory cell scores for poly(catechol-MMA-OEG) and poly(catechol-MMA-OEG) + crosslinker system at **(a)** 72 h, **(b)** 4 weeks, and **(c)** 12 weeks. * represents statistical significance with $p < 0.05$.

5. CONCLUSIONS

In this study, we investigated the *in vivo* biocompatibility of a mussel-mimetic water-soluble adhesive, poly(catechol-MMA-OEG), alone and in conjunction with a sodium periodate crosslinker. Histology of the injection site exhibited heavy macrophage infiltration and presence of neutrophils for both adhesive systems. The heavy macrophage and neutrophil infiltration observed in the injection site of poly(catechol-MMA-OEG) resolved over the course of 12 weeks; however, these cells persisted even at 12 weeks in the injection site of poly(catechol-MMA-OEG) + crosslinker. Both adhesives were not completely resorbed and were still present as a colorless palpable material after 12 weeks. However, both the adhesive systems exhibited signs of mild degradation over the course of time. Since the adhesive did not degrade completely within the time frame studied here (12 weeks), future directions will involve subcutaneous injection of the adhesive for longer time points to enable complete degradation and analysis of any systemic effects from adhesive degradation products. In the case of both adhesives, the kidneys of some mice contained multifocal corticomedullary congestion. As an individual finding, the corticomedullary congestion is unlikely adverse but could potentially be the result of some adhesive degradation from hydrolytic/enzymatic action or from autoclaving. Mild liver necrosis was also observed in one of the mice; however, its cause is unknown. In the future, alternative sterilization methods, such as gamma irradiation, will be explored to prevent effects related to adhesive degradation prior to injection. To provide further context, future studies could compare the biocompatibility of our adhesive systems to the biocompatibility of currently available FDA-approved tissue adhesives or mice that did not receive any test article. Detailed biocompatibility

studies, such as those described here, can help bring us closer to having viable surgical adhesives that prevent the damage caused by mechanical joinery methods.

6. ACKNOWLEDGMENTS

This project was funded with support from the Indiana Clinical and Translational Sciences Institute, which is funded in part by Award Number UM1TR004402 from the National Institutes of Health, National Center for Advancing Translational Sciences, Clinical and Translational Sciences Award (J.J.W). The authors also acknowledge funding from the Purdue Davidson School of Chemical Engineering (J.C.L. and A.V.M.), Purdue Department of Chemistry (J.J.W. and A.V.M.), National Science Foundation grant DMR-2104783 (J.C.L. and J.J.W.), Office of Naval Research grants N000-14-19-1-2342 and N000-14-22-1-2408 (J.J.W.), and a Lillian Gilbreth Postdoctoral Fellowship from Purdue University (A.V.M.). This work was completed in collaboration with the Pre-Clinical Research Laboratory and the Histology Research Laboratory, which are both part of the Center for Comparative Translational Research (College of Veterinary Medicine, Purdue University). Robyn McCain provided help and guidance with experiments. Histological specimens were prepared by Victor Bernal-Crespo.

7. CONFLICT OF INTEREST

J. J. W. is a co-inventor on US Patent No. 10,513,641, and J. J.W. and A. A. P. are co-inventors on CA Patent No. 03084142, which describes the poly(catechol-MMA-OEG) polymer.

REFERENCES

(1) Bal-Ozturk, A.; Cecen, B.; Avci-Adali, M.; Topkaya, S. N.; Alarcin, E.; Yasayan, G.; Li, Y. C. E.; Bulkurcuoglu, B.; Akpek, A.; Avci, H.; Shi, K.; Shin, S. R.; Hassan, S. Tissue Adhesives: From Research to Clinical Translation. *Nano Today* **2021**, *36*, 101049. https://doi.org/10.1016/J.NANTOD.2020.101049.

(2) Nam, S.; Mooney, D. Polymeric Tissue Adhesives. *Chem Rev* **2021**, *121* (18), 11336–11384. https://doi.org/10.1021/ACS.CHEMREV.0C00798.

(3) Ma, Z.; Bao, G.; Li, J. Multifaceted Design and Emerging Applications of Tissue Adhesives. *Adv Mater* **2021**, *33* (24), 2007663. https://doi.org/10.1002/ADMA.202007663.

(4) Duan, W.; Bian, X.; Bu, Y. Applications of Bioadhesives: A Mini Review. *Front Bioeng Biotechnol* **2021**, *9*, 716035. https://doi.org/10.3389/FBIOE.2021.716035.

(5) Bao, Z.; Gao, M.; Sun, Y.; Nian, R.; Xian, M. The Recent Progress of Tissue Adhesives in Design Strategies, Adhesive Mechanism and Applications. *Mater. Sci. Eng. C* **2020**, *111*, 110796. https://doi.org/10.1016/J.MSEC.2020.110796.

(6) Delroisse, J.; Kang, V.; Gouveneaux, A.; Santos, R.; Flammang, P.; Delroisse, J.; Flammang, · P; Kang, V.; Gouveneaux, A.; Santos, R. Convergent Evolution of Attachment Mechanisms in Aquatic Animals. In *Convergent Evolution: Animal Form and Function*.; Cham: Springer International Publishing, **2023**, 523–557. https://doi.org/10.1007/978-3-031-11441-0_16.

(7) Heinritz, C.; Ng, X. J.; Scheibel, T. Bio-Inspired Protein-Based and Activatable Adhesion Systems. *Adv Funct Mater* **2023**, 2303609. https://doi.org/10.1002/ADFM.202303609.

(8) Rao, Y.; Wan, G. Sustainable Adhesives: Bioadhesives, Chemistries, Recyclability, and Reversibility. *Adv Struct Adhes Bonding* **2023**, 953–985. https://doi.org/10.1016/B978-0-323-91214-3.00008-9.

(9) Menezes, A.; Douglas Melo Coutinho, H.; Gonçalves Wanderley, A.; Ribeiro-Filho, J.; Melrose, J. High Performance Marine and Terrestrial Bioadhesives and the Biomedical Applications They Have Inspired. *Molecules* **2022**, *27* (24), 8982. https://doi.org/10.3390/MOLECULES27248982.

(10) Lutz, T. M.; Kimna, C.; Casini, A.; Lieleg, O. Bio-Based and Bio-Inspired Adhesives from Animals and Plants for Biomedical Applications. *Mater Today Bio* **2022**, *13*, 100203. https://doi.org/10.1016/J.MTBIO.2022.100203.

(11) Mu, Y.; Sun, Q.; Li, B.; Wan, X. Advances in the Synthesis and Applications of Mussel-Inspired Polymers. *Polym Rev* **2022**, *63* (1), 1–39. https://doi.org/10.1080/15583724.2022.2041032.

(12) Taghizadeh, A.; Taghizadeh, M.; Yazdi, M. K.; Zarrintaj, P.; Ramsey, J. D.; Seidi, F.; Stadler, F. J.; Lee, H.; Saeb, M. R.; Mozafari, M. Mussel-Inspired Biomaterials: From Chemistry to Clinic. *Bioeng Transl Med* **2022**, *7* (3), e10385. https://doi.org/10.1002/BTM2.10385.

(13) Xie, C.; Li, Y.; Guo, X.; Ding, Y.; Lu, X.; Rao, S. Mussel-Inspired Adhesive Hydrogels for Local Immunomodulation. *Mater Chem Front* **2023**, *7* (5), 846–872. https://doi.org/10.1039/D2QM01232D.

(14) Westwood, G.; Horton, T. N.; Wilker, J. J. Simplified Polymer Mimics of Cross-Linking Adhesive Proteins. *Macromolecules* **2007**, *40* (11), 3960–3964. https://doi.org/10.1021/MA0703002.

(15) North, M. A.; Del Grosso, C. A.; Wilker, J. J. High Strength Underwater Bonding with Polymer Mimics of Mussel Adhesive Proteins. *ACS Appl Mater Interfaces* **2017**, *9* (8), 7866–7872. https://doi.org/10.1021/ACSAMI.7B00270.

(16) Meredith, H. J.; Jenkins, C. L.; Wilker, J. J. Enhancing the Adhesion of a Biomimetic Polymer Yields Performance Rivaling Commercial Glues. *Adv Funct Mater* **2014**, *24* (21), 3259–3267. https://doi.org/10.1002/ADFM.201303536.

(17) Siebert, H. M.; Wilker, J. J. Deriving Commercial Level Adhesive Performance from a Bio-Based Mussel Mimetic Polymer. *ACS Sustain Chem Eng* **2019**, *7* (15), 13315–13323. https://doi.org/10.1021/ACSSUSCHEMENG.9B02547.

(18) Siebert, H. M.; Wilker, J. J. Improving the Molecular Weight and Synthesis of a Renewable Biomimetic Adhesive Polymer. *Eur Polym J* **2019**, *113*, 321–327. https://doi.org/10.1016/J.EURPOLYMJ.2019.01.063.

(19) Jenkins, C. L.; Siebert, H. M.; Wilker, J. J. Integrating Mussel Chemistry into a Bio-Based Polymer to Create Degradable Adhesives. *Macromolecules* **2017**, *50* (2), 561–568. https://doi.org/10.1021/ACS.MACROMOL.6B02213.

(20) Brennan, M. J.; Kilbride, B. F.; Wilker, J. J.; Liu, J. C. A Bioinspired Elastin-Based Protein for a Cytocompatible Underwater Adhesive. *Biomaterials* **2017**, *124*, 116–125. https://doi.org/10.1016/J.BIOMATERIALS.2017.01.034.

(21) Lin, C. Y.; Liu, J. C.; Liu, J. C. Comparison between Catechol- And Thiol-Based Adhesion Using Elastin-like Polypeptides. *ACS Appl Bio Mater* **2020**, *3* (6), 3894–3905. https://doi.org/10.1021/ACSABM.0C00431.

(22) Hollingshead, S.; Torres, J. E.; Wilker, J. J.; Liu, J. C. Effect of Cross-Linkers on Mussel- and Elastin-Inspired Adhesives on Physiological Substrates. *ACS Appl Bio Mater* **2022**, *5* (2), 630–641. https://doi.org/10.1021/ACSABM.1C01095.

(23) Meredith, H. J.; Wilker, J. J. The Interplay of Modulus, Strength, and Ductility in Adhesive Design Using Biomimetic Polymer Chemistry. *Adv Funct Mater* **2015**, *25* (31), 5057–5065. https://doi.org/10.1002/ADFM.201501880.

(24) Putnam, A. A.; Wilker, J. J. Changing Polymer Catechol Content to Generate Adhesives for High versus Low Energy Surfaces. *Soft Matter* **2021**, *17* (7), 1999–2009. https://doi.org/10.1039/D0SM01944E.

(25) Al-Husinat, L.; Jouryyeh, B.; Sharie, S. Al; Modanat, Z. Al; Jurieh, A.; Hseinat, L. Al; Varrassi, G. Bone Cement and Its Anesthetic Complications: A Narrative Review. *J Clin Med* **2023**, *12* (6), 2105. https://doi.org/10.3390/JCM12062105.

(26) Nathanael, A. J.; Oh, T. H. Biopolymer Coatings for Biomedical Applications. *Polymers* **2020**, *12* (12), 3061. https://doi.org/10.3390/POLYM12123061.

(27) Díez-Pascual, A. M. PMMA-Based Nanocomposites for Odontology Applications: A State-of-the-Art. *Int J Mol Sci* **2022**, *23* (18), 10288. https://doi.org/10.3390/IJMS231810288.

(28) Yao, X.; Qi, C.; Sun, C.; Huo, F.; Jiang, X. Poly(Ethylene Glycol) Alternatives in Biomedical Applications. *Nano Today* **2023**, *48*, 101738. https://doi.org/10.1016/J.NANTOD.2022.101738.

(29) Kesharwani, P.; Bisht, A.; Alexander, A.; Dave, V.; Sharma, S. Biomedical Applications of Hydrogels in Drug Delivery System: An Update. *J Drug Deliv Sci Technol* **2021**, *66*, 102914. https://doi.org/10.1016/J.JDDST.2021.102914.

(30) Shi, J.; Yu, L.; Ding, J. PEG-Based Thermosensitive and Biodegradable Hydrogels. *Acta Biomater* **2021**, *128*, 42–59. https://doi.org/10.1016/J.ACTBIO.2021.04.009.

(31) Yang, J.; Cohen Stuart, M. A.; Kamperman, M. Jack of All Trades: Versatile Catechol Crosslinking Mechanisms. *Chem Soc Rev* **2014**, *43* (24), 8271–8298. https://doi.org/10.1039/C4CS00185K.

(32) *ISO - ISO 10993-11:2006 - Biological evaluation of medical devices — Part 11: Tests for systemic toxicity*. https://www.iso.org/standard/35977.html (accessed 2022-03-13).

(33) *ISO - ISO 10993-10:2021 - Biological evaluation of medical devices — Part 10: Tests for skin sensitization*. https://www.iso.org/standard/75279.html (accessed 2022-03-13).

(34) *ISO - ISO 10993-6:2016 - Biological evaluation of medical devices — Part 6: Tests for local effects after implantation*. https://www.iso.org/standard/61089.html (accessed 2022-03-13).

(35) *ISO - ISO 10993-1:2018 - Biological evaluation of medical devices — Part 1: Evaluation and testing within a risk management process*. https://www.iso.org/standard/68936.html (accessed 2022-03-14).

(36) *ISO - ISO 10993-2:2006 - Biological evaluation of medical devices — Part 2: Animal welfare requirements*. https://www.iso.org/standard/36405.html (accessed 2022-03-14).

(37) Lee, H.; Lee, B. P.; Messersmith, P. B. A Reversible Wet/Dry Adhesive Inspired by Mussels and Geckos. *Nature* **2007**, *448* (7151), 338–341. https://doi.org/10.1038/NATURE05968.

(38) Wang, X.; Gu, X.; Yuan, C.; Chen, S.; Zhang, P.; Zhang, T.; Yao, J.; Chen, F.; Chen, G. Evaluation of Biocompatibility of Polypyrrole in Vitro and in Vivo. *J Biomed Mater Res A* **2004**, *68* (3), 411–422. https://doi.org/10.1002/JBM.A.20065.

(39) Zhu, W.; Yang, J.; Iqbal, J.; Peck, Y.; Fan, C.; Wang, D. A. A Mussel-Inspired Double-Crosslinked Tissue Adhesive on Rat Mastectomy Model: Seroma Prevention and in Vivo Biocompatibility. *J Surg Res* **2017**, *215*, 173–182. https://doi.org/10.1016/J.JSS.2017.03.020.

(40) Rincón, A. C.; Molina-Martinez, I. T.; De Las Heras, B.; Alonso, M.; Baílez, C.; Rodríguez-Cabello, J. C.; Herrero-Vanrell, R. Biocompatibility of Elastin-like Polymer Poly(VPAVG) Microparticles: In Vitro and in Vivo Studies. *J Biomed Mater Res A* **2006**, *78A* (2), 343–351. https://doi.org/10.1002/JBM.A.30702.

(41) Li, L.; Stiadle, J. M.; Levendoski, E. E.; Lau, H. K.; Thibeault, S. L.; Kiick, K. L. Biocompatibility of Injectable Resilin-Based Hydrogels. *J Biomed Mater Res A* **2018**, *106* (8), 2229–2242. https://doi.org/10.1002/JBM.A.36418.

(42) Zhu, W.; Peck, Y.; Iqbal, J.; Wang, D. A. A Novel DOPA-Albumin Based Tissue Adhesive for Internal Medical Applications. *Biomaterials* **2017**, *147*, 99–115. https://doi.org/10.1016/J.BIOMATERIALS.2017.09.016.

(43) Yang, Q.; Tang, L.; Guo, C.; Deng, F.; Wu, H.; Chen, L.; Huang, L.; Lu, P.; Ding, C.; Ni, Y.; Zhang, M. A Bioinspired Gallol-Functionalized Collagen as Wet-Tissue Adhesive for Biomedical Applications. *Chem Eng J* **2021**, *417*, 127962. https://doi.org/10.1016/J.CEJ.2020.127962.

(44) Torres, J. E.; Hollingshead, S.; Boucher, D.; & Liu, J. C. Biomimetic Adhesives for Clinical Applications. In *Biomimetic Protein Based Elastomers: Emerging Materials for the*

Future; Royal Society of Chemistry, **2022**, 210. https://doi.org/10.1039/9781788012720-00210.

(45) Lee, S.-H.; Park, C.-W.; Lee, S.-G.; Kim, W.-K. Postoperative Cervical Cord Compression Induced by Hydrogel Dural Sealant (DuraSeal®). *Korean J Spine* **2013**, *10* (1), 44. https://doi.org/10.14245/KJS.2013.10.1.44.

(46) Thavarajah, D.; De Lacy, P.; Hussain, R.; Redfern, R. M. Postoperative Cervical Cord Compression Induced by Hydrogel (DuraSeal): A Possible Complication. *Spine* **2010**, *35* (1). https://doi.org/10.1097/BRS.0B013E3181B9FC45.

(47) Brubaker, C. E.; Kissler, H.; Wang, L. J.; Kaufman, D. B.; Messersmith, P. B. Biological Performance of Mussel-Inspired Adhesive in Extrahepatic Islet Transplantation. *Biomaterials* **2010**, *31* (3), 420–427. https://doi.org/10.1016/J.BIOMATERIALS.2009.09.062.

(48) Brubaker, C. E.; Messersmith, P. B. Enzymatically Degradable Mussel-Inspired Adhesive Hydrogel. *Biomacromolecules* **2011**, *12* (12), 4326–4334. https://doi.org/10.1021/BM201261D.

(49) Soleymani Eil Bakhtiari, S.; Bakhsheshi-Rad, H. R.; Karbasi, S.; Tavakoli, M.; Hassanzadeh Tabrizi, S. A.; Ismail, A. F.; Seifalian, A.; RamaKrishna, S.; Berto, F. Poly(Methyl Methacrylate) Bone Cement, Its Rise, Growth, Downfall and Future. *Polym Int* **2021**, *70* (9), 1182–1201. https://doi.org/10.1002/PI.6136.

(50) Ginebra, M. P.; Montufar, E. B. Cements as Bone Repair Materials. In *Bone Repair Biomaterials: Regeneration and Clinical Applications, Second Edition* **2019**, 233–271. https://doi.org/10.1016/B978-0-08-102451-5.00009-3.

(51) Suzuki, R.; Kuroyanagi, Y. Safety and Utility of a PMMA-Based Tissue Adhesive for Closure of Surgical Incision Wounds. *J Biomater Sci Polym Ed* **2013**, *24* (3), 287–300. https://doi.org/10.1080/09205063.2012.690276.

(52) Jamahiriya, A.; Siddharth Gosavi, S.; Yuvraj Gosavi, S.; Krishna Alla, R. Local and Systemic Effects of Unpolymerised Monomers. *Dent Res J (Isfahan)* **2010**, *7* (2), 82. http://drj.mui.ac.ir/index.php/drj/article/view/299 (accessed 2024-01-05).

(53) Becker, L. C.; Bergfeld, W. F.; Belsito, D. v; Hill, R. A.; Klaassen, C. D.; Liebler, D. C.; Marks, J. G.; Shank, R. C.; Slaga, T. J.; Snyder, P. W.; Andersen, F. A. Final Report of the Cosmetic Ingredient Review Expert Panel Safety Assessment of Polymethyl Methacrylate (PMMA), Methyl Methacrylate Crosspolymer, and Methyl Methacrylate/Glycol Dimethacrylate Crosspolymer. *Int J Toxicol* **2011**, *30(3_suppl)*, 54S-65S. https://doi.org/10.1177/1091581811407352.

(54) Meng, H.; Li, Y.; Faust, M.; Konst, S.; Lee, B. P. Hydrogen Peroxide Generation and Biocompatibility of Hydrogel-Bound Mussel Adhesive Moiety. *Acta Biomater* **2015**, *17*, 160–169. https://doi.org/10.1016/J.ACTBIO.2015.02.002.

(55) Sawyer, D. T.; Valentine, J. S. How Super Is Superoxide? *Acc Chem Res* **1981**, *14* (12), 393–400. https://doi.org/10.1021/AR00072A005.

(56) Mochizuki, M.; Yamazaki, S. I.; Kano, K.; Ikeda, T. Kinetic Analysis and Mechanistic Aspects of Autoxidation of Catechins. *Biochim Biophys Acta Gen Subj* **2002**, *1569* (1–3), 35–44. https://doi.org/10.1016/S0304-4165(01)00230-6.

(57) Lent, E. M.; Crouse, L. C. B.; Eck, W. S. Acute and Subacute Oral Toxicity of Periodate Salts in Rats. *Regul Toxicol Pharmacol* **2017**, *83*, 23–37. https://doi.org/10.1016/J.YRTPH.2016.11.014.